THERMAL ANALISYS FOR A DOUBLE SIDED LINEAR INDUCTION MOTOR

Costica Nituca, PhD

"Gheorghe Asachi" Technical University of Iasi, Romania

Abstract

The paper presents an analysis of the thermal regime for a double sided linear induction motor with ring windings and plate armature. The motor can operate in an oscillating drive system with fast response and low distance movement or for small and medium movement application. A thermal model is realized for the linear induction motor and it is compared with experimental data regarding the thermal aspects.

Keywords: Double sided linear induction motor, thermal, modeling, simulation

Introduction

The linear induction motors are known as solutions for transport vehicles such as urban vehicles or trains, or for linear drives where they can replace the rotary electric machines, hydraulic or pneumatic equipments with linear movement. Thermal regime of the linear induction motor is an important factor during operation because the overheating can affect the structure, the winding insulation and finally, the drive operation. The thermal regime depends on the supply system characteristics, on the driven kinematics, as well as on the linear motor structure and on its cooling system. The need for an analysis of the thermal processes can arise when designing a linear motor (Sarapulov & Goman 2009) but also for the supplying system and for the protection of the system (Plesca 2010)**,** (Plesca 2011)**.**

In some situations, to improve the thermal behavior, an insulation layer is used. By placing the insulation layer between the primary part of the machine, the temperature difference and temperature fluctuation in the machine due to varying motor load are reduced (Eun 2003). The linear induction motor can be used in the automotive suspension system (Hyniova 2012), where a three-phase linear motor is used, with a limitation for the maximum temperature of 100 ^{o}C. The main advantage of the solution is the possibility to generate desired forces acting between the unsprung (wheel) and sprung (one-quarter of the car body

mass) masses of the car, providing good insulation of the car sprung mass from the road surface roughness and load disturbances.

An original application of the linear motor can be the wave-energy conversion, as a part of the effort for the renewable energy development (Danson 2008). Moreover, double-sided designs increase the air-gap of the machine, linking more flux than single-sided machines.

Some systems must have high performance such as high precision and high speed. It is therefore important to analyze, design and control linear motor used widely as an actuator in the precision stage. For a double-sided linear motor with yoke and multi-segmented array, the coating on the coil cannot stand the temperature more than 120 ^{o}C (Lee 2006).

Thermal analyses can be conducted by means of analytical or numerical methods. The analytical method based on lumped parameters is faster, but its accuracy depends on the level of refinement of the thermal network and on the knowledge of the heat transfer coefficients (Amoros 2011). The objective is to check that, within the specified conditions of operation, the temperature rise in the different parts of the motor does not surpass the limit value of the chosen insulation class.

In order to avoid the complex conjugate problem, convection heat transfer within fluid flow and conduction within solid parts were modeled and solved separately. As an alternative approach, a simple one-dimensional thermal resistance model was introduced and compared with the finite element analysis.. The influences of some factors, such as thermal conductivity of the insulation sheet, thermal contact between the coil assembly and the mounting plate, and air-cooling or water-cooling were examined through the analysis (Jang 2003).

Linear motors can be used as efficient tool to achieve the high speed and accuracy. However, a high speed feed drive system with linear motors, in turn, can generate heat problems. Also, frictional heat is produced at the ball or roller bearing of the linear motor block when driven at high speed. It can affect the thermal deformation of the linear scale as well as that of the machine tool structure. The thermal deformation characteristics can be identified through measuring the thermal error caused from thermal deformation of the linear scale and the machine tool structure (Kim 2004).

Another possible application of the linear induction motor is to drive the pantograph collecting system for the electric vehicles, like trains and tramways (Nituca 2003). In this case the motor assures the contact force for the contact between the catenary and the contact line. Moreover, its control assures a better contact and improve the current collection process

and reduces the wear of the pantograph and of the contact line and reduce the detachments of the pantograph skate from the wire (Nituca 2007).

The end effects are the particular sensitive difficulty to model the linear drives. The 3D magnetic and thermal models are achieved taking into account the end effects and the metaphysical aspects of a linear motor studied as a braking system with different displacement velocities. The startup thrust force is studied with the coupling between the magnetic and thermal models (Jinlin 2010).

A linear motor is a direct drive system which is a heat source and placed near to the working area. Therefore, this thermal effect characteristic study is conducted here to find out the effect of heat that is transferred and dissipated around the working area, causing unwanted deformation. The surface area joining the linear motor coil to the application carriage is large. It will be inaccurate to assume a constant temperature or heat flux through the entire surface. The temperature of the surface is different for different location and time (Chow, J.H. 2010).

The construction of the linear induction motor with ring windings

The linear motor considered (Fig. 1) is a three-phase one, double sided, with a vertical plate mobile armature (1) from copper. On the two inductors (2a and 2b), there are placed the ring windings in 24 slots, yielding the coils (3). The air gap δ is to be found on the both sides of the plate armature, the total air gap being 2·δ. The mobile armature has an oscillating movement (4) on a distance of about 0÷250 mm.

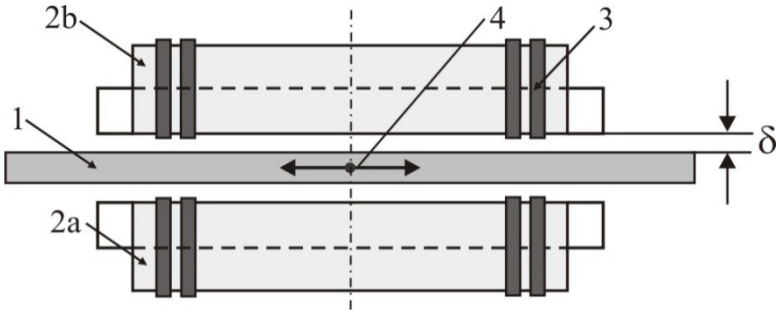

Fig. 1. The double sided linear induction motor.

For the small oscillating movements (less than 100 mm), the plate armature will be almost all the time in the same relative position with respect to the inductors, which will give a higher heating and consequently a modification of the machine's parameters. In fact, such regime may yield to an overheating of the windings and of the armature plate which can result in insulation melting, short-circuit of the winding, the armature deformation and thus to the damage of the motor. This transient regime can affect the protection system as fuses or circuit breakers **(**Plesca 2010**).**

Determining the temperature distribution, highlights the parameters that govern the critical zones and possibly optimize the cooling system to meet the constraints and standards imposed. (Bertin, Y. - 2010). Therefore, the estimation of the temperature of the windings can be made by indirect method (using a mathematical relationship (Valcov 2009, Livint & Stan 2001)), or by direct method (using specific devices for the temperature measurement and monitoring (Livint & Stan 2001, Scintee & Plesca 2009). Finite element method is also used for heat transfer analysis in three-phase linear motor (Huang 2010) and thermal resistance is studied for different applications of the linear motor, as in (Jang 2003).

The heating differential equation for the linear motor

The linear motors are more difficult to study from the thermal point of view in comparison with the rotary motors because of their specific construction and the related electromagnetic process. The thermal estimations need to evaluate the losses in the windings and in conducting materials. An analysis can be made, for a first estimation, in analogy with the rotary machines starting from the thermal equation:

$$Qdt = A\theta dt + Cd\theta \tag{1}$$

Thus, the heat Q released into the machine in a dt time is equal to the heat released by the machine for a difference of temperature θ between the machine and the environment ($A\theta dt$), plus the heat absorbed by the machine ($Cd\theta$) to increase its temperature by θ degrees. The equation (1) can be rewritten as:

$$(Q - A\theta)dt = Cd\theta, \tag{2}$$

or

$$dt = \frac{Cd\theta}{Q - A\theta}; \tag{2'}$$

where:

- C is the thermal capacity of the machine;
- A is the heat transfer capacity of the machine.

The integration of the equation (2') will give the variation relationship of the machine heating (Botan 1970):

$$\theta = \frac{Q}{A}\left(1 - e^{-\frac{t}{C/A}}\right) + \theta_0 e^{-\frac{t}{C/A}}, \tag{3}$$

where θ_0 is the initial temperature of the machine; if it is equal to the environment temperature, it can be considered as the temperature axis origin. The relation (3) shows the maximum temperature:

$$\theta_{\max} = \frac{Q}{A} \tag{4}$$

The ratio C/A is a constant for a given machine and represents the time constant of the machine heating or the temperature delay (thermal inertia) of the machine:

$$T_\theta = \frac{C}{A} \tag{5}$$

As a value, the heating time constant T_θ is the necessary time for the machine to reach the θ temperature by releasing the heat in the environment, where:

$$\theta = 0.632\theta_{\max} \tag{6}$$

The time constant of the heating T_θ is obtained as in Fig. 2. The intersection between the tangent and the temperature θ_{max} gives the time constant T_θ.

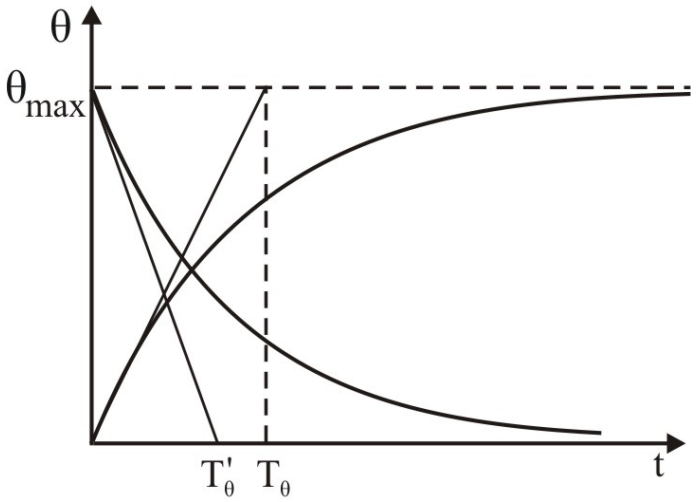

Fig. 2. The heating curve and the cooling curve of the machine.

It is to notice that if the temperature of the motor is equal to the temperature of the environment, the relation (3) becomes:

$$\theta = \frac{Q}{A}\left(1 - e^{\frac{t}{T_\theta}}\right) \tag{7}$$

If the motor is stopped and the power is switched off, the motor starts to cool and the variation of the temperature is given by the equation:

$$\theta = \theta_{\max} e^{-\frac{t}{T_\theta'}} \tag{8}$$

where T_θ' is the time constant of the cooling, which is usually different from the time constant of the heating (Fig. 2).

Thermal modelling of the double sided linear induction motor

For a better understanding of the thermal aspects of the linear motor, it was realized a model and simulations of the thermal regime. Fig. 3 presents the geometrical model of the linear induction motor with the armature plate of copper and the two modules of the inductors. The inductors are symmetrically on the plate with an air gap of 1 mm. Fig. 3 presents a detail for a single inductor, with the notations: 1-the mobile plate armature; 2-inductors; 3-windings; 4-yokes. The data used for the thermal simulation are:

- for the mobile plate armature (from copper): material density: 8900 kg/m3, specific heat: 385 J/kggrd.C, thermal conductivity: 385 W/mgrd.C;
- for the yokes (iron): density: 7190 kg/m3, specific heat (thermal capacity): 420.27 J/kggrd.C, heat (thermal) conductivity: 52.028 W/mgrd.C;
- For the insulation: density: 1400 kg/m3, specific heat (thermal capacity): 137 J/kggrd.C, heat (thermal) conductivity: 1.25 W/mgrd.C.

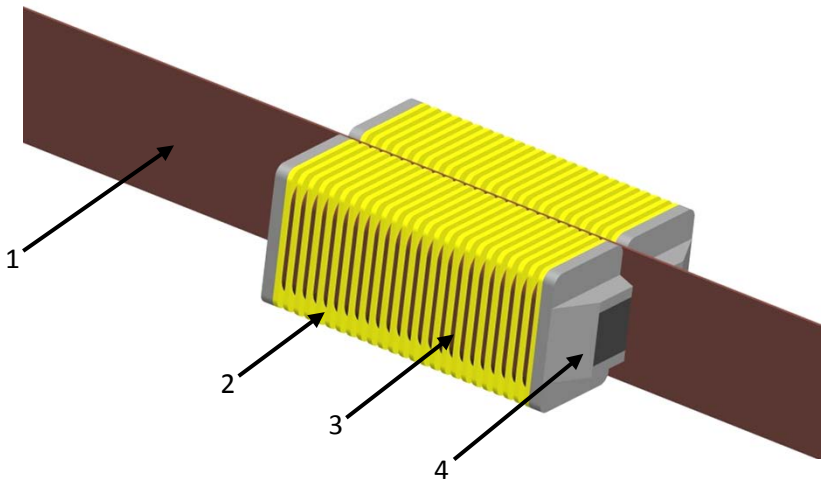

Fig. 3. Geometrical model of the linear induction motor: 1-mobile plate armature; 2- inductors; 3-windings; 4- yoke.

Figure 4 presents the thermal distribution for the linear induction motor for a 20 ^{o}C ambient temperature. It is to see that the maximum temperature is in the middle of the inductors and it is about 92.4 ^{o}C, very close to the experimental measurements, as presented below.

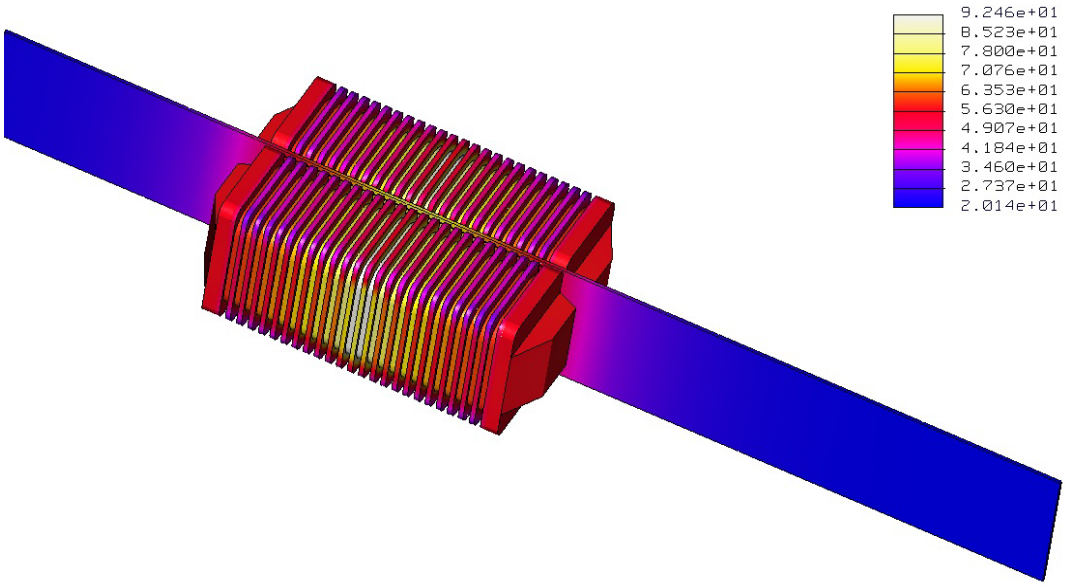

Fig. 4 Thermal distribution for the double sided linear induction motor.

Figure 5 presents a section through the linear motor to see the plate armature and only one inductor. The maximum temperatures are in the middle on the copper windings, with values of about 90 ^{o}C, and on the lateral windings the temperature is about 60 ÷ 62 ^{o}C. On the armature plate the distribution of the temperatures is from about 85 ^{o}C in the middle to about 30 ^{o}C on the edges.

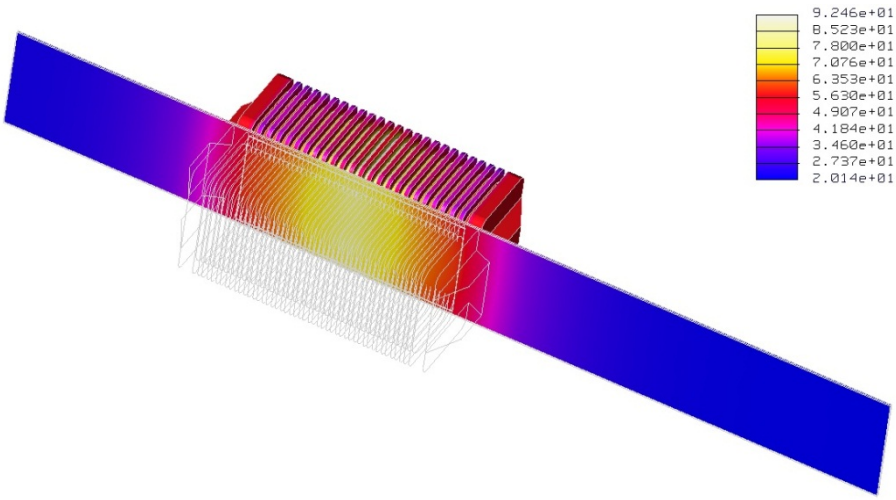

Fig. 5. Thermal distribution of the linear induction motor - section through motor.

The thermal load was distributed uniformly in all the volume of every copper winding. On the lateral areas the temperature is lower because the windings are in contact with the lateral pieces of aluminum, which have a coefficient of convection of 19.75 W/m ^{o}C. For the inductor the coefficient is 14.2 W/m ^{o}C and for the isolation it was considered 12.5 W/m ^{o}C.

Experimental thermal tests of the linear induction motor

The estimation of the temperature increase of the windings and of the other parts of the motor is made with a locked armature. The inductor is supplied, for the first tests, at rated voltage and rated frequency from a three-phase symmetrical supply system (by a three-phase autotransformer). For the second test the motor is supplied by an alternative voltage variator. The supply schema is given in figure 6.

The temperature is measured with an infrared thermometer CA876 with laser aiming in the range -20°C...+550°C, and 1°C acuity and a precision of about ± 2%. The choice of sensor location is not simple. It depends on access to areas of the machine during its construction (Glises 2010).

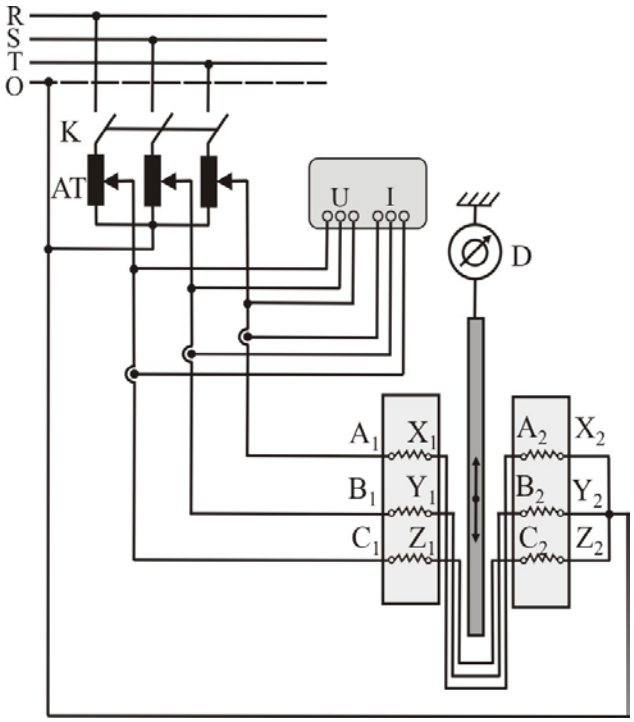

Fig. 6. The supply schema of the linear induction motor for the thermal regime analysis

The temperature measurement points on the linear motor are presented in figure 7. On the mobile armature plate (1) the temperatures were measured in points θ_1 and θ_2 at the edges of the plate and between the inductors 2a and 2b. For the coils the temperature is measured in point θ_3 at the 13th coil of the inductor 2a and in point θ_4 on the 14th coil of the inductor 2b because these are the coils with maximum temperatures. For the yokes 3a and 3b, the temperature is measured at the points θ_5, θ_6, θ_7, θ_8. All of these will give a large view over the variation of the temperature in the motor.

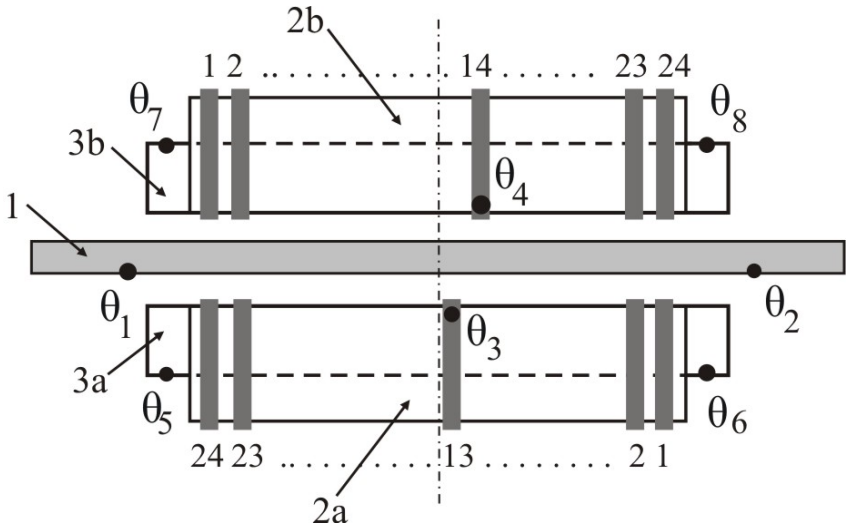

Fig. 7. The measurement points for the temperature of the linear induction motor.

The measured temperatures with the motor supplied from an autotransformer are presented in Table 1. For a current of I = 1.25 A and voltage of 275 V, the force is F = 40 N. The motor is supplied for 70 minutes and the temperature is measured every 10 minutes. The higher temperatures are measured on the two inductors, and a medium value is measured in yokes and low temperatures are measured on the armature plate extremities.

Table 1. Measured temperatures in different point of the motor for a force of 40 N

Time [Min]	$\theta_{armature}$ [C^o]		$\theta_{inductors}$ [C^o]		θ_{yoke} [C^o]			
	θ_1	θ_2	θ_3	θ_4	θ_5	θ_6	θ_7	θ_8
0	23	23	23	23	23	23	23	23
10	26	26	36	38	31	30	28	31
20	27	27	41	44	37	36	33	38
30	27.5	27.7	45	49	40	41	35	43
40	28	28.2	51	54	43	43	37	44
50	28.5	30	55	58	45	47	40	47
60	29	30.5	56	60	48	50	44	51
70	29.5	31	61.5	63	53	54	47	56

Because the maximum temperatures are for the inductor coils, it is necessary to estimate the time constant of the heating T_θ for the machine, using the relations (3-6). We obtain T_θ = 850 [s], the maximum estimated temperature being θ_{max} = 60 ^{o}C. With these data and using the relation (3), we obtain the heating curve of the linear motor (Fig. 8 where the curve 1 is the experimental one and the curve 2 is determined by the relation (3)).

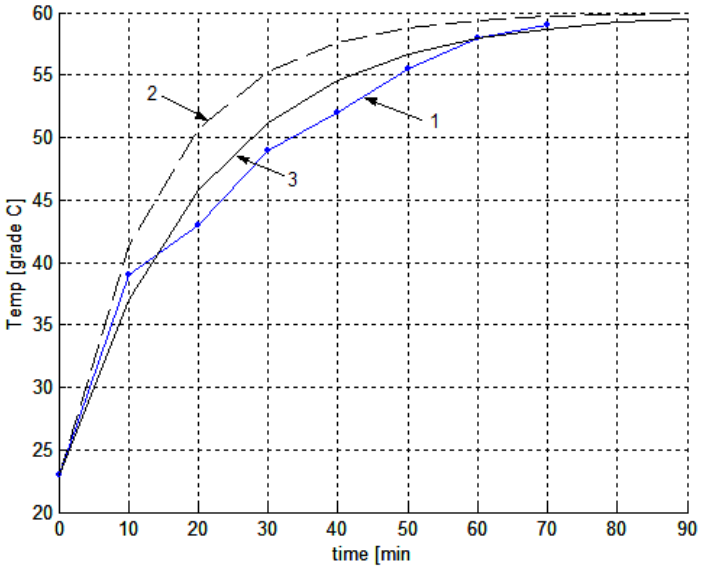

Fig. 8. The heating curves of the inductor number 2 with autotransformer supply.

The curve 2 describes with a good precision the experimental curve only for the beginning and for the end of the curve, which is explained by the incorrect value of the time constant of the heating. By some correction it is obtained the curve (3) which is more precise for the entire curve, the time constant of the heating being of T_θ = 1250 [s], corresponding for a 42 ^oC temperature, that is 0.7 from the maximum temperature. Thus, the relation (6) can be revised as $\theta = 0.7 \cdot \theta max$.

Similar analyses were performed with the linear motor supplied by an alternative voltage variator (Table 2). The situation is different from the above case because of the current harmonics which could lead to higher heating of the semiconductor devices (Plesca 2011, chapter in book).

The maximum temperatures are also for the inductor coils, the time constant of the heating being of T_θ = 870 [s], for an estimated maximum temperature θ_{max} = 66 ^oC. Figure 9 presents the experimental variation heating curve 1 and the estimated curve 2 (using the relation (3)).

Table 2. Measured temperatures at different points of the motor supplied by a voltage variator

Time [Min]	$\theta_{armature}$ [C^o]		$\theta_{inductors}$ [C^o]		θ_{yoke} [C^o]			
	θ_1	θ_2	θ_3	θ_4	θ_5	θ_6	θ_7	θ_8
0	25	25	25	25	25	25	25	25
10	27	27	36	40	31	30	28	31
20	27.5	27.5	41	45	37	37	33	36
30	27.8	27.7	45	49.5	40	41	35	42
40	28	28.1	51	54.5	42	43	37	44
50	28.5	29	55	58	45	47	40	47
60	29	39	56	60	49	50	45	51
70	29	31	61	63	53	54	48	55

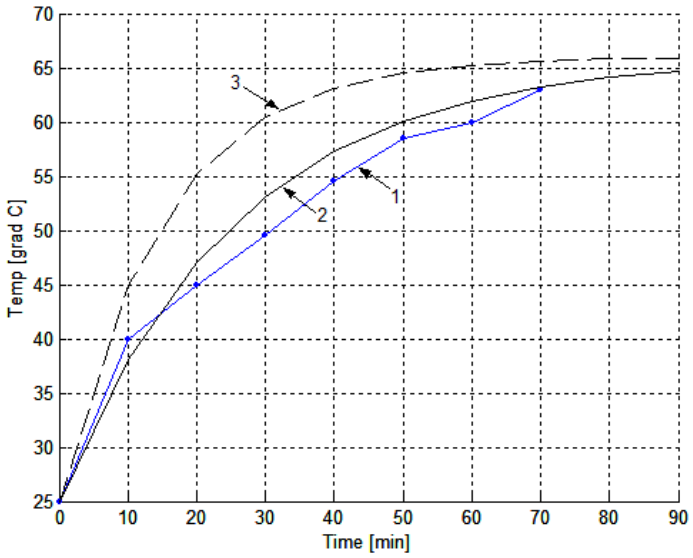

Fig. 9. The heating curves of the inductor number 2 with voltage variator supply.

As above, there are necessary corrections which give the heating curve 3, the time constant of the heating being of $T_{(}$ = 1550 [s], corresponding to a 47 ^{o}C temperature, that is 0.711 from the maximum temperature. Thus, the expression (6) can be revised as:

$$\theta = 0.711 \cdot \theta_{max} \quad (9)$$

Conclusion

A study of the heating phenomena for a double sided linear induction motor with armature plate and ring windings is presented. There were estimated the relationships for the temperature variation in the maximum temperature points. It was realized a correction of the graphical estimation of the time constant of the heating which allows a more precise heating curve estimation for different situations and different points.

A thermal model for the linear induction motor is realized in order to estimate the heating area on the motor. From the study it results that the theoretical characteristics of the motor heating overlap in the experimental characteristics.

References:

Amorós J.G., Andrada P., and Blanqué B., “Design procedure for a longitudinal flux flat linear switched reluctance motor”, Electric Power Components and Systems, 40:161–178, 2012.

Botan, N., “Bazele acţionărilor electrice”, Editura Tehnica Bucuresti, 1970.

Chow, J.H.; Zhong, Z.W.; Lin, W.; Khoo, L.P.; Lin, W.J.; Yang, G.L., “Investigation of thermal effect in permanent magnet linear motor stage”, 11th International Conference on Control, Automation, Robotics and Vision, ICARCV 2010,p 258-262,2010.

Danson M. Joseph and Willem A. Cronje, "Design of a double-sided tubular permanent-magnet linear synchronous generator for wave-energy conversion", COMPEL: The International Journal for Computation and Mathematics in Electrical and Electronic Engineering, Vol. 27 No. 1, 2008 pp. 154-169.

Ung E.I., "Effects of insulation layer upon the thermal behavior of linear motors", KSME International Journal, Vol. 17 No. 6, pp. 896 ~ 905, 2003.

Glises, R., "Machines électriques tournantes Simulation du comportement thermique", www.techniques-ingenieur.fr, October 2010.

Huang, DS., Shih, JS., Hsia, HC., Lin, MT.,"Three-Phase linear motor heat transfer analysis using the finite-element Method", Heat Transfer Engineering, 31(7), 617-624, 2010.

Hyniova K., Krajl M. and Smitkova-Janku L., "Experiments on energy management in active suspension of vehicles", International Journal Of Systems Applications, Engineering & Development Issue 2, Volume 6, 2012.

Jang, C., Kim, JY., Kim, YJ., Kim, JO., "Heat transfer analysis and simplified thermal resistance modeling of linear motor driven stages for SMT applications", IEEE Transactions on Components and Packaging Technologies, 26(3), 532-540, 2003.

Jinlin G., Gillon F., Brochet P., "Magnetic and thermal 3D finite element model of a linear induction motor", 2010 IEEE Vehicle Power and Propulsion Conference, VPPC 2010.

Jang, C; Kim, JY; Kim, YJ; Kim, JO, "Heat transfer analysis and simplified thermal resistance modeling of linear motor driven stages for SMT applications", IEEE Transactions on Components and Packaging Technologies, vol. 26, pp. 532-540, 2003.

Kim Jong-Jin , Jeongb Young Hun, Cho Dong-Woo, "Thermal behavior of a machine tool equipped with linear motors, International Journal of Machine Tools and Manufacture", Vol. 44, Issues 7–8, Pages 749–758, 2004.

Lee M.G., Choi Y.M., Lee Sung Q., Lim D.C, Gweon D.G., "Design of high precision linear stage with double-sided multi-segmented trapezoidal magnet array and its compensations for force ripples", Mechatronics 16 (2006) 331–340.

Livinţ, P., Stan, Gh., "Sistem computerizat pentru studiul regimului termic al motorului asincron trifazat", A III-a Conferinţă Internaţională de Sisteme Electromecanice şi Energie, Chişinău, R. Moldova, Vol. I, pp. 95-98, 2001.

Niţucă C., Cantemir L., Gheorhgiu A., Chiriac G., "Pantograph drived with a linear induction motor controlled with adaptive fuzzy control", The 4th International Conference on Electromechanical and power systems SIELMEN 2003, Vol III, pg. 55-58, Chişinău 26-27 september 2003.

Niţucă C., Rachid A., Cantemir L., Chiriac G., Gheorghiu A., "Constructive and experimental aspects regarding the electric power collecting for very high speed train", 6th International Conference on Electromechanical and Power Systems SIELMEN 2007, Analele Univ. din Craiova, Anul 31, vol. II, pp. 290-293, 2007.

Pleşca, A., "Thermal Analysis of Power Semiconductor Converters", Book Chapter in Power Quality Harmonics Analysis and Real Measurements Data, Ed. Intech, Croatia, 20 pg., 2011.

Plesca, A., "Busbar temperature monitoring and correlation with protection electrical apparatus", International Review of Electrical Engineering (IREE), vol.6, n.5, pp.2659-2665, Sep – Oct 2011.

Plesca, A., "Thermal analysis of fuses and busbar connections at different type of load variations", International Review on Modelling and Simulations (IREMOS), vol.3, n.5, Part B, pp.1077-1086, October 2010.

Plesca, A., "Thermal transient regime analysis for fuses and power semiconductors", International Review on Modelling and Simulations (IREMOS), vol.3, n.5, Part B, pp.1070-1076, October 2010.

Sarapulov, F. N. and Goman, V. V., 2009, "'Development of mathematical models of thermal processes in linear asynchronous motors", Russian Electrical Engineering, 2009, Vol. 80, No. 8, pp. 431–435. Allerton Press, Inc., 2009. Original Russian Text F.N. Sarapulov, V.V. Goman, 2009, published in Elektrotekhnika, 8 (2009) 17–21.

Scîntee A., Plesca A., „Installation for testing, adjustment and control of three-phase low voltage automatic ac circuit breakers, with dynamic switching", 3rd International Symposium on Electrical Engineering and Energy Converters, September 24-25, 2009, Suceava.

Vâlcov, N., "Contactless method for temperature measurements of electrical machines windings", Romanian Metrology Revue, No 2, 2009.